

SIMULATING HYDRAULIC FRACTURING PROCESSES IN CEMENT COMPOSITES USING TOUGH-RBSN

DAISUKE ASAHINA^{*}, MIKIO TAKEDA[†], AND KOHEI NAGAI^{††}

^{*} Geological Survey of Japan, AIST

AIST Tsukuba center 7, 1-1-1 Higashi, Tsukuba, Ibaraki, 305-8567, Japan

e-mail: d-asahina@aist.go.jp, www.aist.go.jp

[†] Geological Survey of Japan, AIST

AIST Tsukuba center 7, 1-1-1 Higashi, Tsukuba, Ibaraki, 305-8567, Japan

e-mail: mikio-takeda@aist.go.jp

^{††} The University of Tokyo

4-6-1 Komaba, Meguro-ku, Tokyo, 153-8505, JAPAN

e-mail: nagai325@iis.u-tokyo.ac.jp, www.u-tokyo.ac.jp

Key words: Pore pressure, Hydraulic fracture, Hydro-mechanical processes, Rigid-body-spring network (RBSN)

Abstract: This paper presents the coupled hydro-mechanical simulation tool, TOUGH-RBSN, to investigate fundamental aspects of hydraulic fracture of cement-based composites. The TOUGH-RBSN simulator is based on the effective linking of two numerical methods: TOUGH2, a finite volume method for simulating mass transport within a permeable medium; and a lattice model based on the rigid-body-spring network (RBSN) concept. The material is represented as a three-phase composite consisting of a mortar matrix, coarse aggregate inclusions, and matrix-inclusion interfaces. Local fracture permeabilities and porosities are based on the crack apertures computed by the mechanical model. The simulator is used to study the effects of weak interfaces on the hydraulic fracturing processes.

1 INTRODUCTION

Elevated fluid pressure within pores and cracks in cement composites induces mechanical condition changes and potentially affects their durability. An understanding of hydromechanical interactions associated with microcrack formation in cement composites is important for structural engineering applications such as the design of high concrete dams, and offshore concrete structures for deep water petroleum production. However, hydraulic conditions of cracked concrete can be difficult to predict, because they depend not only on the appearance of the crack formation, but also on the interactions with pre-existing microcracks and various environmental conditions.

This paper presents recent developments of an existing 3D hydro-mechanical (HM)

simulation tool and the application to hydraulic fracturing simulation of cement composites. The first part of this paper summarizes recent work of the authors, which involves the coupled HM simulation tool, TOUGH-RBSN [1]. TOUGH2 is used to simulate flow and transport through discrete fractures and within porous rocks [2], whereas elasticity and fracture development are simulated by a lattice model based on the Rigid-Body-Spring Network concept [3]. Thereafter, the application to hydraulic fracturing simulations of cement composites is presented. The material is represented as a three-phase composite composed of a mortar matrix, aggregate inclusions, and matrix-inclusion interfaces, which are regarded as a weak link in determining the mechanical properties. The fracture events and their

patterns during a progressive failure process are discussed. The effects of matrix-inclusion interfaces on the hydraulic fracturing process are also presented.

2 SIMULATION APPROACH

A brief overview is given for the existing codes TOUGH2, a multiphase flow and transport simulator developed at the Lawrence Berkeley National Laboratory [2], and RBSN, which is used to model the elasticity and fracture development of geomaterials [4]. The linkage of TOUGH2 to RBSN is also briefly described in this section. Additional model details can be found in the literature [1, 5, 6].

2.1 Hydrological model: TOUGH2 simulator

TOUGH2 is a widely used general-purpose numerical simulator for non-isothermal flows of multiphase, multicomponent fluids in permeable and fractured geomaterial. The integral finite difference (or finite volume) method is used as the numerical solution scheme. In this paper, the simulations of flow are based on the TOUGH2 with the EOS1 equation-of-state module, which accounts for water present in liquid, vapor, and two-phase. The TOUGH2 related study can be found elsewhere [2]; only unique arrangement of discrete fracture representation is described here [5].

The authors have developed an approach within TOUGH2 to represent discrete fractures in permeable porous geomaterials [1, 5]. As shown in Figure 1a, the matrix is a basic material structure, which is represented by a Voronoi tessellation of a spatially random set of points. A discrete fracture is represented by additional fracture nodes at the Voronoi cell boundaries (Fig. 1b). Additional sets of connections are also introduced with associated nodes to activate flow pathways between fracture and matrix nodes. The crack opening associated with a mechanical element is related to local fracture permeability and porosity.

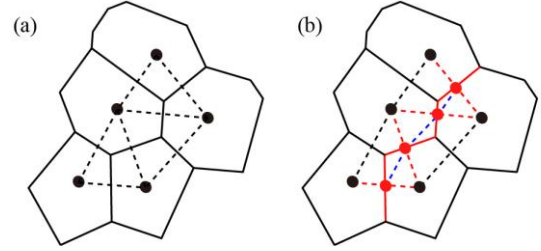
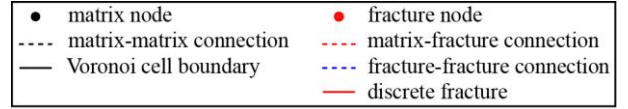


Figure 1: 2D description of nodes and connections in the TOUGH2 simulator: (a) matrix nodes and connections, and (b) additional insertion of fracture nodes and insertion/replacement of fracture connections. (adopted from [1])

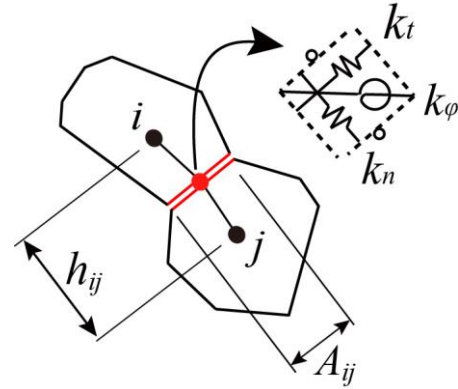


Figure 2: A lattice element defined by nodal connectivity $i-j$ with zero-size spring set located at centroid of surface area A_{ij} .

2.2 Mechanical-damage model: RBSN

The material domain is discretized as a collection of two-node elements, as shown in Figure 2. The dual Delaunay tessellation of the nodal points defines geometry of the rigid-bod-spring network. Each lattice element consists of a zero-size spring set. The spring stiffnesses are set according to $k_n = k_s = k_t = A_{ij}E/h_{ij}$, in which E is the elastic modulus, h_{ij} is the distance between nodes i and j , and A_{ij} is the area of the Voronoi boundary common to nodes i and j (Fig. 2). In this study, the strength properties of a lattice element are defined by the Mohr-Coulomb criterion. Fractures propagate along the Voronoi cell boundaries as HM induced stresses evolve and exceed the strength of the materials.

Asahina et al. (2017) recently developed a novel approach to accurately represent elastic

constants (E and ν), while retaining the simplicity and advantages of using lattice elements [7]. Unlike conventional lattice or discrete models, the elastic constants of a material are represented without any need for calibration.

2.3 Coupling of hydraulic and mechanical damage codes

The general procedure of the two-code coupling, hydraulic and mechanical code, is based on the pioneering work of Rutqvist et al. (2002), whereas the modifications and extensions are made for modeling fracture propagation, as discussed in Asahina et al. (2014). Several capabilities of the coupled TOUGH-RBSN simulator have been demonstrated through simulations of laboratory experiments, as reported in the previous studies [5, 6].

TOUGH2 compute the hydraulic quantities (e.g. fluid pressure, degree of saturation), whereas RBSN calculates the mechanical quantities (e.g., force, displacement, damage index). An external module exchanges these primary quantities between two codes at each time step. In this study, the effective stress is calculated in the conventional law of Biot's theory for porous materials

$$\sigma_n = \sigma'_n + \alpha_P P \quad (1)$$

where σ_n is the total normal stress, σ'_n is the effective stress, α is the Biot effective stress parameter, P is the pressure in the pores. Compressive stress is positive in this study. In incremental form, Eq. (1) can be,

$$\Delta\sigma_n = \Delta\sigma'_n + \alpha_P(\Delta P_i + \Delta P_j)/2 \quad (2)$$

where ΔP_i and ΔP_j are the changes in pore pressures over time step at neighboring nodes i and j . The pore pressure only affects the lattice element in the normal direction. Elastic and failure analysis is conducted with the updated total normal stresses. Thereafter, the mechanical quantities from RBSN are used to update the hydraulic properties associated with the Voronoi cell and boundary in the TOUGH model. The hydraulic properties (i.e., porosity, permeability, and capillary pressure) are functions of the mechanical quantities (i.e.,

effective stress, strain, and damage index) [8]. Data exchanges between two codes are relatively simple since they share the same Voronoi grid and associated set of nodes.

3 HYDRAULIC FRACTURING IN MULTIPHASE PARTICULATE MEDIA

In this study, the TOUGH-RBSN simulator demonstrates hydraulic fracture processes in cement-based composites. The basic model set up is partly taken from Kim et al. (2017) where they conducted planar analyses of hydraulic fracturing in a rock-analog sample (i.e., glass material), which contained designed pre-existing fractures. Consider the Voronoi discretization of a 90 mm square domain with a 3.2 mm injection borehole at the center (Fig. 3). The two models are considered here: a homogeneous material, and a three-phase material that includes a mortar matrix, hard inclusions, and a matrix-inclusion interface. Note that the identical domain discretization is used for both cases as can be seen in Figure 3a and 3b, but the assignment of the element properties is according to phase composition of the concrete [9]. For the homogeneous material, the elastic moduli and the tensile strength are set to 31.6 GPa and 3.46 MPa, respectively. For the three-phase material, the tensile strengths of each component (i.e., aggregate inclusion, matrix, and interface) are assumed to be proportioned according to $f_a : f_m : f_i = 2 : 1 : 0.25$, as representative of normal strength concrete, where the tensile strength of the matrix phase f_m , is set to 8MPa.

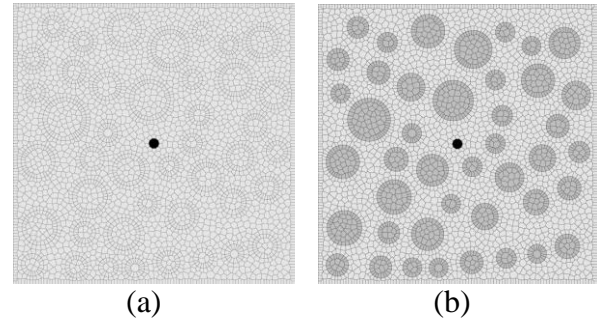


Figure 3: Domain discretization based on the Voronoi tessellation: (a) homogeneous material model, and (b) three-phase material model (dark and light grey represent inclusions and mortar matrix, respectively). The black dot at the center of the domain indicates the location of pressure injection.

Table 1: Hydrological properties of cement composite, fracture, and borehole domains.

	Cement Composite	Fracture	Borehole
Permeability, (m ²)	1.0e-12	$b_h^2/12^*$	1.0e-8
Porosity, (-)	0.2	0.8	0.8
Pore Compressibility, (Pa ⁻¹)	0.0	3.0e-8	5.0e-9

* The permeability of a fracture depends on the hydraulic aperture width, which is evaluated by Eq. (3) with an assumption for the residual hydraulic aperture $b_{hr} = 0.25 \mu\text{m}$ [6].

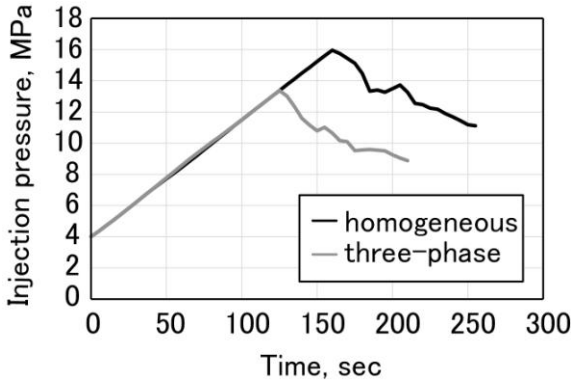


Figure 4: Time evolution of injection pressures simulated for homogeneous, and three-phase material model.

The ratio of the elastic moduli of the aggregate and matrix phase is set at 3:1, with $E_m = 25\text{GPa}$. The slope of the Mohr-Coulomb surface is assumed to be $\varphi = \tan^{-1} 1.0$. The interface strength in direct shear, c , is assumed to be 3MPa . The model is subjected to biaxial loading of 4.83 , and 7.24MPa in the horizontal, and vertical directions, respectively. Table 1 summarizes the hydrological properties. The hydraulic aperture is coupled to the mechanical aperture b_m [10]:

$$b_h = b_{hr} + b_m \quad (3)$$

where b_{hr} is the residual hydraulic aperture. Water is injected into the borehole with the rate of $3.8 \times 10^{-5} \text{cm}^3/\text{s}$ per unit centimeter thickness [6].

Figure 4 shows simulated fluid pressure in the borehole as a function of time. Fluid pressure is linearly increased at the beginning, and the pressure reduces after the first element breakage induced by fluid pressure. The

homogeneous material model shows higher injection pressure than that of the three-phase material model.

3.1 Numerical results: homogeneous material model

Figure 5 shows the simulated fracture patterns of the homogeneous model induced by water injection in early and late stages. Visualization of the damage developments is facilitated by the Voronoi cell boundaries of breaking lattice elements. Hydraulic fractures are initiated from two opposite sides (top and bottom) of the pressurizing borehole. This direction is a normal to the smallest magnitude of principal stresses. The fluid migrates into the newly fractured elements, whose permeabilities and porosities are based on the crack apertures computed by Eq (3).

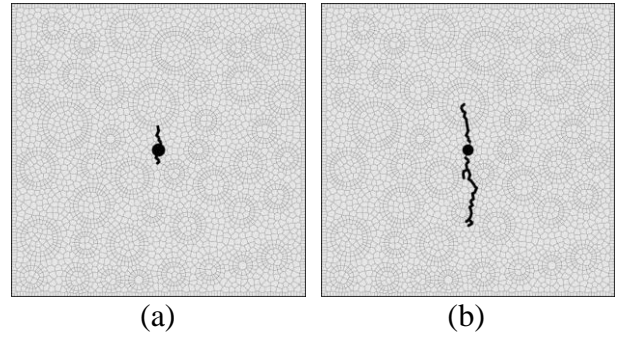


Figure 5: Snapshots of the simulated fracture traces of homogeneous material model: (a) early, and (b) late stage.

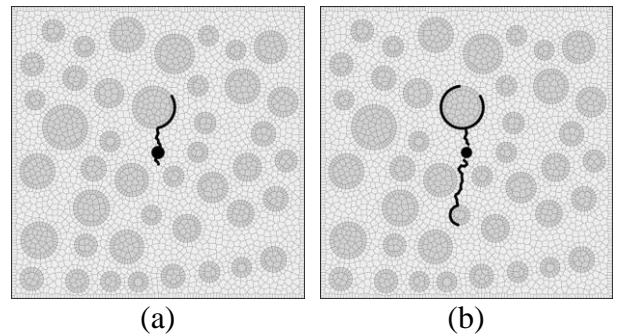


Figure 6: Snapshots of the simulated fracture traces of three-phase material model: (a) early, and (b) late stage.

3.2 Numerical results: three-phase material model

Figure 6 shows the simulated fracture patterns of the three-phase material model.

Although hydraulic fractures initiate from two opposite sides of the pressurizing borehole, they tend to go around the aggregates along the weak matrix-inclusion interfaces. It can be seen that local direction of cracks is sensitive to the locations of the aggregates and correlates with neighboring aggregates, especially along the direction of the maximum compressive stress (i.e., vertical direction in this study). As a next step, we anticipate conducting the physical experiments to study the effect of the aggregate inclusions on fracture patterns induced by fluid pressure.

4 CONCLUSIONS

The TOUGH-RBSN simulator was used to simulate hydraulic fracture of cement-based composites. Attention has been given to modeling the fracture patterns of composites materials during a progressive failure induced by elevated pore pressure. Although the simulator has been validated against laboratory experiments of geomaterials in the previous studies, additional work is needed to compare the proposed simulation results and physical test results.

The results presented in this paper are part of our ongoing work which involves the study of the durability mechanics of cement-based composites. The presented TOUGH-RBSN simulator appears to be an effective means for analyzing concrete under severe conditions, such as offshore structures for seabed resource developments.

REFERENCES

- [1] Asahina, D., Pan, P., Tsusaka, K., Takeda, M., Bolander, J.E., 2018. Simulating hydraulic fracturing processes in laboratory-scale geological media using three-dimensional TOUGH-RBSN. *Journal of Rock Mechanics and Geotechnical Engineering*. 106:1102-11.
- [2] Pruess, K., Oldenburg, C., Moridis, G. TOUGH2 User's Guide, Version 2. Lawrence Berkeley National Laboratory, 2011.
- [3] Kawai, T., 1978. New discrete models and their application to seismic response analysis of structures. *Nuclear Engineering and Design*. 481:207-29.
- [4] Bolander, J.E., Saito, S., 1998. Fracture analyses using spring networks with random geometry. *Engineering Fracture Mechanics*. 615-6:569-91.
- [5] Asahina, D., Houseworth, J.E., Birkholzer, J.T., Rutqvist, J., Bolander, J.E., 2014. Hydro-mechanical model for wetting/drying and fracture development in geomaterials. *Computers & Geosciences*. 65:13-23.
- [6] Kim, K., Rutqvist, J., Nakagawa, S., Birkholzer, J., 2017. TOUGH-RBSN simulator for hydraulic fracture propagation within fractured media: Model validations against laboratory experiments. *Computers & Geosciences*. 108:72-85.
- [7] Asahina, D., Aoyagi, K., Kim, K., Birkholzer, J.T., Bolander, J.E., 2017. Elastically-homogeneous lattice models of damage in geomaterials. *Computers and Geotechnics*. 81:195-206.
- [8] Rutqvist, J., Tsang, C.-F., 2002. A study of caprock hydromechanical changes associated with CO₂ -injection into a brine formation. *Environmental Geology*. 422-3:296-305.
- [9] Asahina, D., Landis, E.N., Bolander, J.E., 2011. Modeling of phase interfaces during pre-critical crack growth in concrete. *Cement and Concrete Composites*. 339:966-77.
- [10] Rutqvist, J., Noorishad, J., Tsang, C.-F., Stephansson, O., 1998. Determination of fracture storativity in hard rocks using high-pressure injection testing. *Water Resources Research*. 3410:2551-60.